Indoor Simultaneous Localization And Mapping Based On FastSLAM

Xingming Zhu[1, a], Hong Song [1, a], Xisong Gan [2, a]

[1]Sichuan University of Science &Engineering, Yibin 644000, China

[2]Jiangling Holdings Limited Development Center, China

[a]360157107@qq.com

Abstract

Aiming at the disadvantage of the traditional FastSLAM algorithm that the proposed sampling distribution only considers the robot motion model, a more confident lidar observation data is introduced into the sampling distribution of pose estimation by data fusion, which effectively reduces the cumulative error of pose estimation. Then an adaptive resampling method is introduced to reduce the calculation. The SLAM precision is increased with the number of particles. The improved algorithm is tested by MATLAB simulation. In addition, a dynamic global path planning solution based on static A * algorithm of ROS navigation package and DWA algorithm is designed.

Keywords

RBPF; simultaneous localization and map building; path planning.

1. Introduction

The research of mobile robot usually has to solve three basic problems: firstly, the robot estimates its position and pose; secondly, it expresses the environment model by special representation method based on the unfamiliar scene information obtained by the sensor; thirdly, it calculates a safe driving path from the starting point to the target point independently. Simple summary is: self-positioning, map building and path planning, SLAM technology, that is, simultaneous positioning and map building. They are the basis for mobile robots to navigate in unknown situations and complete tasks at the same time. The description of the self-localization problem is to calculate the position coordinates and orientation angles of the robot system in the global map according to the sensor information. Map building refers to the integration of information acquired by system sensors into a specified representation to complete the real environment modeling, which includes various detectable obstacles in the environment. Path planning is to use a specific algorithm in the work environment to find a safe route from the starting point to the target point. The design criteria of path planning algorithms are usually based on three points: the least cost, the shortest path and the least time.

In the research and application of mobile service robots, the robot navigation theory system based on prior environmental information has been developed more mature. But for the dynamic environment and unknown environment, the technology development of autonomous navigation control is still very young, and is still in the exploratory experimental stage. There is still a long way to go to solve the problems of system modeling and path planning under uncertain environmental information. In this paper, the research on mobile service robot technology is mainly based on the indoor environment such as residential and office, relying on the information obtained by robot sensors to achieve positioning, map construction, path planning and other navigation work.

2. Improved FastSLAM algorithm based on RBPF

Theoretical research shows that the closer the proposed distribution is to the target distribution, the better the effect of particle filter is. The proposed distribution of particle sampling based on Rao-Blackwellized particle filter FastSLAM 1.0 is the motion model of the robot, without taking into account the latest observations z_t, that is, no roots. According to the latest observation data, the robot pose is updated in real time, so the deviation between the robot pose represented by each particle and the actual robot pose is larger. When the noise error of the robot motion model is very large, many particles sampled from the proposed distribution will deviate from the actual position and attitude of the robot, which will lead to a large deviation between the final map and the actual environment. If the target distribution can be sampled directly, then the best filtering effect can be obtained. And there is no need for resampling steps. In practice, it is often difficult to sample directly from the target distribution. In order to make the proposed distribution closer to the target distribution, the proposed distribution can be improved by introducing the t-moment observation z_t into the proposed distribution. When the robot's observation sensor accuracy is higher than the robot's control accuracy, the system improvement effect will be different. It is often obvious[1].

The particle representation of the proposed improved particle filter SLAM algorithm is the same as that of the Fast SLAM 1.0 algorithm based on particle filter. The complete update process is as follows:

Pose sampling

In the sampling stage, the latest system observation information is fused into the robot motion model, and the proposed distribution is expressed as follows:

$$x_t^k \sim p(x_t \mid x_{1:t-1}^k, u_{1:t}, z_{1:t}, c_{1:t}) \tag{1}$$

The following improvements are made to the proposed distribution:

$$\begin{aligned} & p(x_t \mid x_{1:t-1}^k, u_{1:t}, z_{1:t}, c_{1:t}) \\ & = \eta^k \left\{ p(z_t \mid m_{c_t}, x_t, c_t)\, p(m_{c_t} \mid x_{1:t-1}^k, z_{1:t-1}, c_{1:t-1}) dm_{c_t}\, p(x_t \mid x_{t-1}^k, u_t) \right. \end{aligned} \tag{2}$$

The first order Taylor expansion is used to approximate the observation function H：

$$h(m_{c_t}, x_t) \approx h(\mu_{c_t,t-1}^k, \overset{-k}{x_t}) + H_m \cdot (m_{c_t} - \mu_{c_t,t-1}^k) + H_x \cdot (x_t - \overset{-k}{x_t}) \tag{3}$$

The following parameters are expressed as follows:

$$\begin{cases} \overset{-k}{z_t} = h(\mu_{c_t,t-1}^k, \overset{-k}{x_t}) \\ \overset{-k}{x_t} = g(x_{t-1}^k, u_t) \\ H_m = \nabla_{m_{c_t}} h(m_{c_t}, x_t) |_{x_t = \overset{-k}{x_t}, m_{c_t} = \mu_{c_t,t-1}^k} \\ H_x = \nabla_{x_t} h(m_{c_t}, x_t) |_{x_t = \overset{-k}{x_t}, m_{c_t} = \mu_{c_t,t-1}^k} \end{cases} \tag{4}$$

H_m and H_x are Jacobian matrices with respect to the observation function h, and are the values of the derivatives of H with respect to m_{c_t} and x_t at the expected values of their parameters. Under this approximation, Gauss, which satisfies the expected sampling and distribution, can be obtained：

$$\Sigma_{x_t}^k = (H_x^T [Q_t^k]^{-1} H_x + [R_t]^{-1})^{-1} \tag{5}$$

$$\mu_{x_t}^k = \Sigma_{x_t}^k H_x^T [Q_t^k]^{-1} (z_t - \overset{-k}{z_t}) + \overset{-k}{x_t} \tag{6}$$

$$Q_t^k = \mathrm{H}_m \Sigma_{c_t,t-1}^k \mathrm{H}_m^t + Q_\mathrm{t} \tag{7}$$

Among them, R_t represents the covariance of the motion noise, and Q_t represents the covariance of the observed noise[2].

Feature estimation update

c_t still represents the correlation variable at time t, n represents the nth characteristic, and when $c_t \neq n$ indicates that the system has not observed the characteristic n at time t, there are:

$$(\mu_{n,t}^{k}, \Sigma_{n,t}^{k}) = (\mu_{n,t-1}^{k}, \Sigma_{n,t-1}^{k}) \tag{8}$$

When $c_t \neq n$, the system observed the characteristic n at t time and updated the environmental characteristics of the K particle：

$$p(m_{c_t} \mid x_t^k, z_{1:t}, c_{1:t}) = \eta\, p(z_t \mid x_t^k, m_{c_t}, c_t)\, p(m_{c_t} \mid x_{1:t-1}^k, z_{1:t-1}, c_{1:t-1}) \tag{9}$$

The measurement function H is first-order Taylor expansion, and x_t is a non-free variable, so the approximate expression is as follows:

$$\begin{aligned} h(m_{c_t}, x_t) &\approx h(\mu_{c_t,t-1}^{k}, \overset{-k}{x_t}) + H_m \cdot (m_{c_t} - \mu_{c_t,t-1}^{k}) + H_x \cdot (x_t - \overset{-k}{x_t}) \\ &\approx \overset{-k}{z_t} + H_m \cdot (m_{c_t} - \mu_{c_t,t-1}^{k}) \end{aligned} \tag{10}$$

At this point:

$$\begin{aligned} & p(x_t \mid x_{1:t-1}^k, u_{1:t}, z_{1:t}, c_{1:t}) \\ & = \eta \cdot \exp\left\{ -\frac{1}{2}(z_t - \overset{-k}{z_t} - H_m \cdot (m_{c_t} - \mu_{c_t,t-1}^{k}))Q_t^{-1}\,(z_t - \overset{-k}{z_t} - H_m \cdot (m_{c_t} - \mu_{c_t,t-1}^{k})) \right. \\ & -\frac{1}{2}(m_{c_t} - \mu_{c_t,t-1}^{k})[\Sigma_{c_t,t-1}^{k}]^{-1}(m_{c_t} - \mu_{c_t,t-1}^{k}) \end{aligned}$$

(11)

Feature updating is achieved by extending Calman filtering：

$$\Sigma_{c_t,t}^{k} = (I - K_t^K \cdot H_m)\Sigma_{c_t,t-1}^{k} \tag{12}$$

$$K_t^k = \Sigma_{c_t,t-1}^{k} H_m^T (Q_t)^{-1} \tag{13}$$

$$\mu_{c_t,t}^{k} = \mu_{c_t,t-1}^{k} + K_t^K (z_t - \overset{-k}{z_t}) \tag{14}$$

The new particles after the estimation of new features are added to the temporary particle set.

Resampling:

To execute (1) (2) processes for all particles, a temporary set of M particles is obtained. Determining resampling importance coefficient:

$$\begin{aligned} w_t^k &= \frac{p(x_t^k \mid z_{1:t}, u_{1:t}, c_{1:t})}{p(x_t^k \mid z_{1:t}, u_{1:t}, c_{1:t}, x_{1:t-1}^k)\, p(x_{1:t-1}^k \mid z_{1:t-1}, u_{1:t-1}, c_{1:t-1})} \\ &= \eta \int p(x_t \mid x_{t-1}^k, u_t) \int p(z_t \mid m_{c_t}, x_t, c_t) \\ & p(m_{c_t} \mid x_{1:t-1}^k, z_{1:t-1}, c_{1:t-1}, u_{1:t-1})\, dm_{c_t}\, dx_t \end{aligned} \tag{15}$$

η is the normalization constant, and finally the importance coefficient is deduced as follows：

$$w_t^k \approx \eta \cdot |2\pi L_t^t|^{-\frac{1}{2}} \cdot \exp\left\{ -\frac{1}{2}(z_t - \overset{-k}{z_t})^T [L_t^t]^{-1} (z_t - \overset{-k}{z_t}), \right. \tag{16}$$

$$L_t^t = H_x^T Q_T H_x + H_m \Sigma_{c_t,t-1}^{k} H_m^T + R_T$$

By normalizing the importance coefficient of resampling, and then resampling, a new particle set with pose and map information can be obtained.

3. Adaptive resampling

For particle filter, the weight variance of particles generated by sequential importance sampling method will increase with time, causing particle degradation.. "Particle degeneration" refers to the increasing variance of the weights of the particle set after many times of meditation, in which only a few particles have larger weights and most of the other particles have smaller weights. At this time, a large number of calculations are used to update the nearly useless particles with small weights. Theory has proved that particle degeneration is unavoidable, which greatly wastes computational resources. The resampling process effectively prevents the particle degradation process, and more high-weight particles are chosen to replace low-weight particles. However, frequent resampling will lead to the problem of particle depletion, that is, the particles with high weights are replicated many times, those with low weights are ignored, and the particles are concentrated near a few points with large posterior probability value, thus losing the diversity of particles[3].

Grisetti also uses an adaptive resampling algorithm to measure the degree of particle degradation by calculating the effective particle number N_{eff} . The smaller the N_{eff} value, the greater the variance of the weight of the particle, the more serious the degree of particle degradation[4]. On the contrary, it shows that the better the particle diversity: the approximate expression of N_{eff} is as follows:

$$N_{eff} = \frac{1}{\sum_{i=1}^{N} (w_k^{(i)})^2} \tag{17}$$

In the formula, N represents the number of particles: w_k^i is the normalized weight of particles. $N_{eff} \leq N/2$ is usually set to the time system to re-sampling process. Through a large number of experiments, it is found that this method can effectively reduce the risk of particle degradation. Because the number of resampling decreases, it is only executed when needed. By introducing the adaptive resampling method, the number of resampling and the complexity of the algorithm can be effectively reduced, and the robustness of the algorithm can be improved.

4. Simulation verification

In order to verify the effectiveness of the proposed algorithm, the improved FastSLAM algorithm based on raster map is implemented on MATLAB simulation platform. Fig. 2 is a simulated indoor environment. The experimental environment is a labyrinth of approximately 21 m * 23 m with 10 rasters per meter. As shown in Figure 2, the robot completes both positioning and incremental raster mapping in the environment, where black lines represent the interior walls.

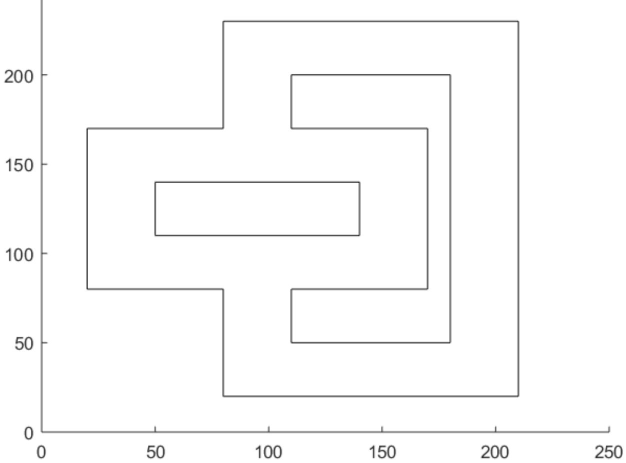

Fig. 1 Simulated experimental environment

Figure 1 depicts the incremental creation of raster maps on the initial map during the mobile robot movement.

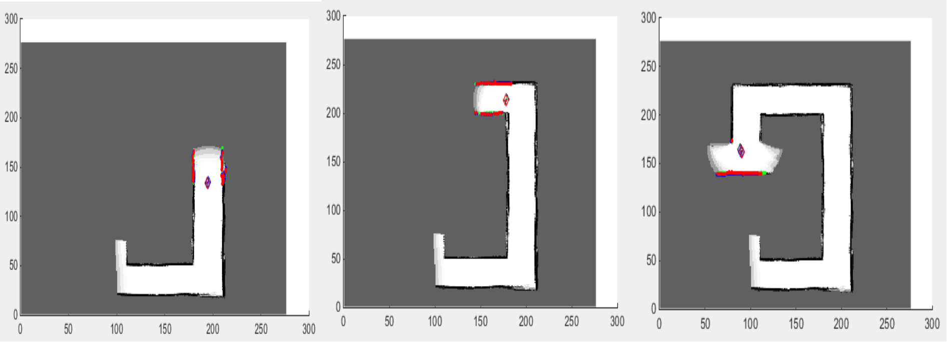

Fig. 2 Drawing process

The purple-red diamond represents the robot, the dark blue represents the grid map created by laser scanning, the red represents the corridor boundary (obstacles), and the sky blue represents the boundary of laser scanning at this time.

In the experiment, the number of particles is 30, and the number of effective particles is 15. This process completely simulates the construction of a mobile robot with a laser rangefinder scanner in a real environment.Fig. 3 (a) and (b) represent robot pose errors in the traditional Fast SLAM algorithm based on raster maps and in the improved Fast SLAM algorithm based on raster maps, respectively.

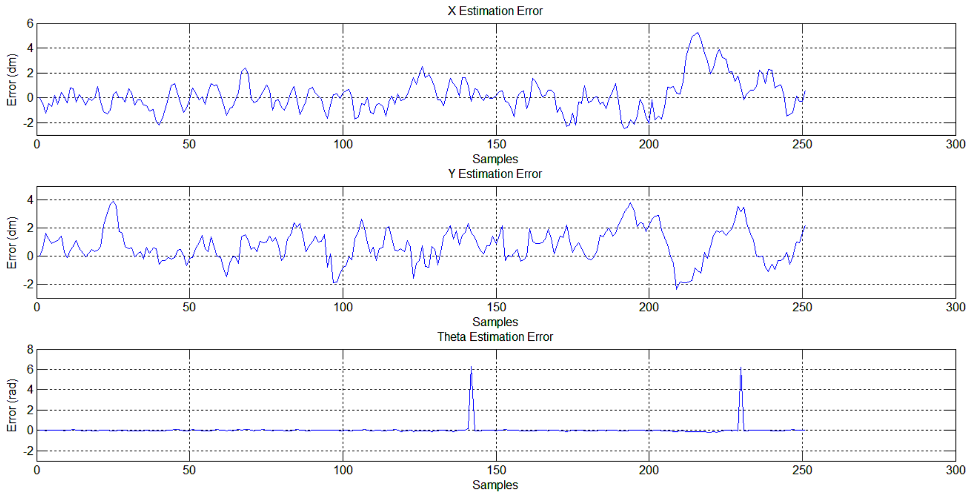

Fig. 3 (a)

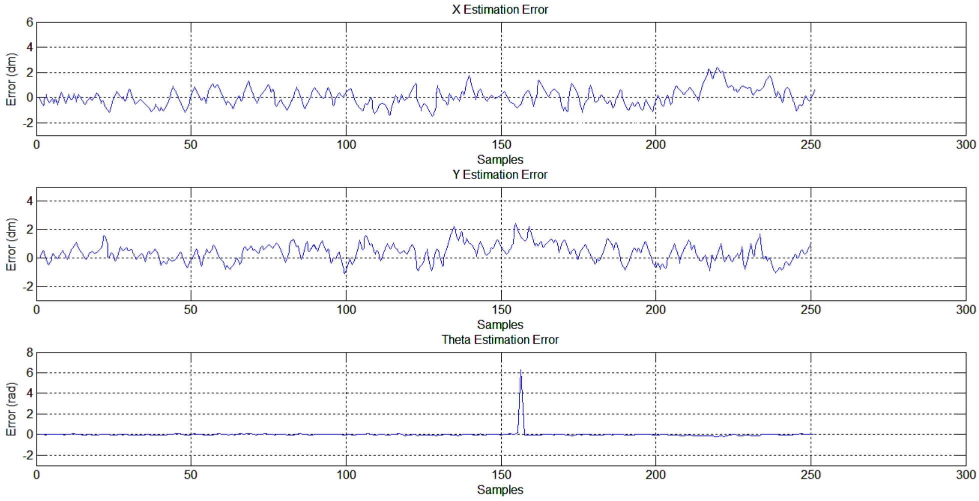

Fig. 3 (b)

Fig. 3 Comparison of pose estimation error

From the Fig.3 (a), it can be seen that the robot position error is approximately between 0-6 cm and the yaw angle error is between 0.2-0.5 rad. The robot positioning effect is poor because the grid map precision is related to the robot positioning. When the robot positioning is not accurate, it will cause map errors. The difference is large. From the Fig.3 (b), it can be seen that the robot position error is approximately between 0-2 cm, and the yaw angle error is approximately between 0-0.1 rad. Compared with the traditional algorithm, the robot positioning effect is better, so the established map is closer to Figure 2.

5. Robot indoor SLAM experiment

In this experiment, the raspberry pie uses the Ubuntu mate operating system, and the ROS version used in the Ubuntu mate is Kinetic. In the experiment, two computers are used. The raspberry pie 3B is used as the airborne PC control robot. It is responsible for the implementation of SLAM algorithm and navigation. The airborne PC communicates with X-2 experimental platform and laser radar through serial port and USB interface. As a remote control PC, notebook computer controls and monitors the experimental process of robot through virtual machine and rviz visualization. The communication mechanism between the robot platform and the PC control platform is as follows:

Set up the VMware network mode to bridge the WiFi network card from windows.

Enter the robot Ubuntu system and access the same WiFi with PC windows.

In PC virtual machine ubuntu, two computers need to be configured in a ROS environment to run ROS MASTER on the raspberry pie host. Therefore, the environment variables ROS_MASTER_URI in raspberry pie and virtual machine are configured as http:/(robot ip): 11311, and their ROS_HOSTNAME is configured as their respective I. P.

Using SSH service to realize remote login raspberry pie 3B Ubuntu system, you can write, compile and run ROS code through a notebook.

The real environment selected in this paper is 427 Laboratory of Artificial Intelligence Experiment Center of Sichuan University of Light Chemical Technology. The length and width of the laboratory are 8 meters each. The length and width of the corridor are 12 meters and 3 meters respectively. The total area needed to be mapped is 100 square meters. There are two points to pay special attention to before building a map.

When the robot moves through the keyboard, it avoids the emergence of sudden stop and acceleration to avoid collision between the robot and obstacles, resulting in pose drift.

Rotate a certain angle remotely at a complex position with more feature points to obtain a larger scanning angle of the lidar, so as to make the mapping operation more adequate and reduce the probability of the area not being scanned in the map.

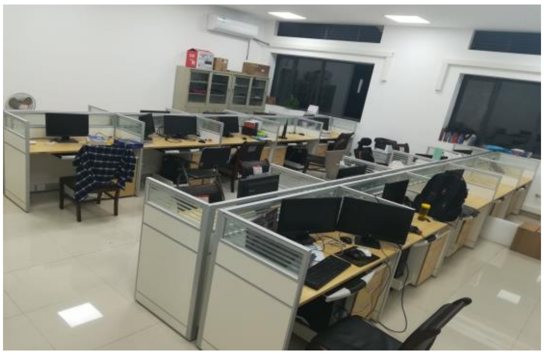

Fig. 4 Posture change relation of robots at adjacent time

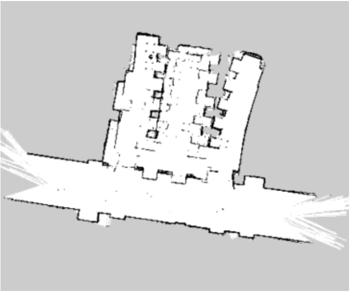

Fig. 5（a)

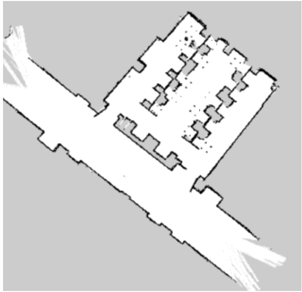

Fig. 5（b)

As shown in Fig. 6, for the result of the map creation experiment using SLAM, the graph (a) is the result of using only the robot motion model, and the graph (b) is the result of introducing high-precision observational measurement to correct the pose while considering the motion model in the proposed distribution. Considering the cumulative error caused by mechanical noise, when the mapping process is scanned to the repetitive area, the generated map drifts obviously. When the new proposed distribution is improved and repeated experiments are carried out under the same conditions, the results of the map construction are very clear and tidy, and also tally with the actual scene.

In the FastSLAM algorithm based on particle filter, robot localization is realized by particle maintenance. During the SLAM process, the particles representing the map are measured continuously. The map displayed each time is the highest weight among all the particles representing the map. Through the continuous modification in the whole SLAM process, the final weight is obtained. The position and pose estimation of the largest particle completes the closed loop to realize the map construction, so the positioning accuracy of the system directly determines the mapping construction effect. As a result, the more particles the system maintains, the higher the positioning accuracy of the robot will be, and the map construction will be more accurate. But in practice, the hardware conditions and the scene complexity will affect the positioning accuracy. The influence of excessive particle number is that the system calculation load is too high, which will lead to poor or even failure in the final mapping. Therefore, under different conditions, we need to choose the most appropriate particle number range through experiments.

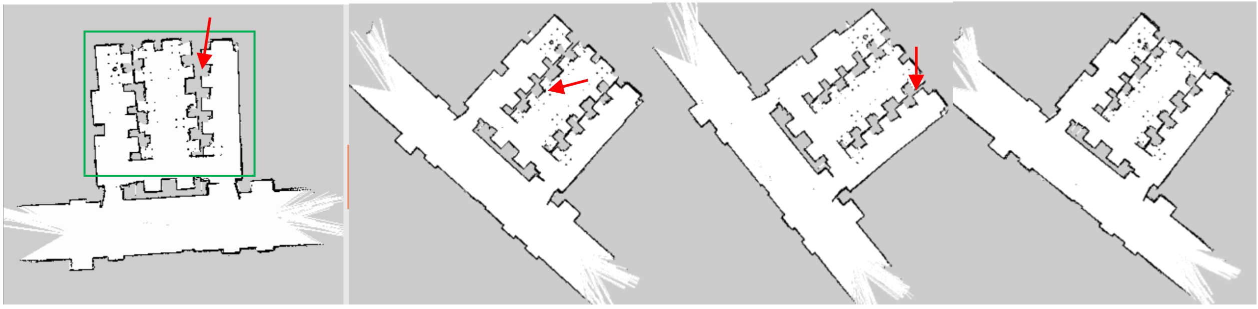

Fig. 6 Different particle mapping experiments

As shown above, the map is constructed when the number of particles is 20, 40, 100, and 30 respectively. The green box in the map is the laboratory interior, the red arrow is the desk placed horizontally close to each other, the black dot represents various small diameter obstacles such as chair legs, and the yellow arrow represents the wall, which is compared with the real scene. It can be found that when the number of particles is 20, the desks placed side by side (at the red arrow) produce greater separation, and the map contour is somewhat distorted and unclear. When the number of particles is 40 and 100, although the map sharpness is improved, there is still a close desk in the map separation phenomenon, only when the number of particles is 30, the construction of the desk. The boundary of the map boundary is clear without scattering, and the desk is close to the actual scene.

References

[1] Paine N, Mehling J S, Holley J, et al. Actuator control for the NASA‐JSC Valkyrie humanoid robot: A decoupled dynamics approach for torque control of series elastic robots[J]. Journal of Field Robotics, 2015, 32(3): 378-396.

[2] Choi T, Do H, Kim G, et al. An example of performing art with robot[C]//Ubiquitous Robots and Ambient Intelligence (URAI), 2016 13th International Conference on. IEEE, 2016: 905-906.

[3] Subramanian M B, Sudhagar K, Rajarajeswari G. Design of navigation control architecture for an autonomous mobile robot agent[J]. Indian Journal of Science and Technology, 2016, 9(10).

[4] Lin P, Abney K, Bekey G A. Robot ethics: the ethical and social implications of robotics[M]. The MIT Press, 2014